energy&fuels

pubs.acs.org/EF Article

Ex Situ and *In Situ* Thermal Transformations of M-50 Pitch Revealed by Non-contact Atomic Force Microscopy

Pengcheng Chen, Jordan N. Metz, Adam S. Gross, Stuart E. Smith, Steven P. Rucker, Nan Yao,* and Yunlong Zhang*

Cite This: *Energy Fuels* 2021, 35, 18210−18219 Read Online

ACCESS | Metrics & More | Article Recommendations | Supporting Information

ABSTRACT: Petroleum pitch M-50 (or A-240) has been well-known in making valuable carbon materials through thermal treatments. How these molecules react to produce carbon materials and the mechanisms of thermal polymerization and molecular weight growth under thermal conditions are of great significance and yet still unclear. Structures produced by thermal reactions of M-50 pitch were characterized with non-contact atomic force microscopy and compared to the structures in M-50 pitch previously characterized (Chen, P.; Metz, J. N.; Mennito, A. S.; Merchant, S.; Smith, S. E.; Siskin, M.; Rucker, S. P.; Dankworth, D. C.; Kushnerick, J. D.; Yao, N.; Zhang, Y. Petroleum pitch: Exploring a 50-year structure puzzle with real-space molecular imaging. *Carbon* **2020**, *161*, 456−465, DOI: 10.1016/j.carbon.2020.01.062). Reaction products were generated from M-50 pitch by two different approaches: an *ex situ* approach via thermal treatment at 400 °C under N_2 and an *in situ* approach via reaction directly on a Cu(111) surface. Polycyclic aromatic hydrocarbons (PAHs) from the *ex situ* reaction are larger than those in the starting M-50 pitch and with fewer methyl groups. Both types of five membered rings, conjugated and non-conjugated, are observed. Very large PAHs are formed under the *in situ* surface conditions as a result of reactions catalyzed by the Cu surface, with five-membered rings preserved as planar moieties in the product. The data suggest that methyl groups play important roles in initiating the polymerization and molecular weight growth of M-50 pitch molecules, but the reactivities of five-membered rings remain unclear.

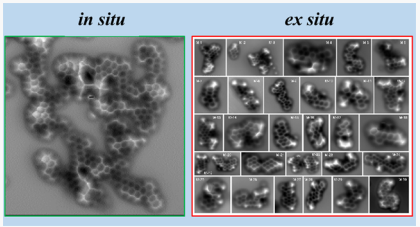

1. INTRODUCTION

M-50 petroleum pitch (also known as A-240 pitch) was produced from the bottoms of the fluidized catalytic cracking process in petroleum refining and is enriched in polycyclic aromatic hydrocarbons (PAHs). It has been well-known that M-50 has properties suitable for producing a mesophase pitch usable for making more valuable carbon materials. Since it was initially reported as early as the 1960s,[1] tremendous effort has been devoted to characterizing the molecules in M-50 pitch,[2−16] and several representative or average structures have been proposed for it (Figure 1a), including the original structures by Dickinson[2,4] and Seshadri et al.[3] based on quantitative nuclear magnetic resonance (NMR) spectroscopy, molecular weight, and elemental analyses.[3,4] Dickinson pointed out that the inconsistencies in the structures proposed by Seshadri et al.[3] on the relatively smaller condensed cores and a predominance of ethylene ($-CH_2CH_2-$) or methylene ($-CH_2-$) linkers were caused by inaccurate quantitative measurements of different kinds of aromatic carbons as a result of insufficient dosing of the relaxation reagent, $Cr(acac)_3$, in the sample,[4] and he contended that the predominant structures were highly condensed aromatic ring systems. In a later analysis, however, Kershaw and Black suggested that one in two molecules contain a ring-joining methylene (RJM) group in a five-membered ring (Figure 1a).[6] Structures with a single linkage via an aryl−aryl bond (Figure 2) were also frequently found in the structures by Dickinson,[4] Lewis, and Mochida et al.[17−19]

The representativeness and utility of average structures is limited by the large diversity of structures in M-50 pitch. A major breakthrough was achieved by Thies and co-authors in the 1990s when M-50 pitch was separated by molecular weight using the dense-gas extraction (DGE) technique, and fractions of monomer, dimer, and trimer were obtained.[5,8,9] More importantly, it was suggested that oligomers are formed by monomers fused via conjugated five-membered rings (Figures 1a and 2) based on detailed analysis of matrix-assisted laser desorption/ionization (MALDI) mass spectrometry (MS) data and comparison to the ultraviolet−visible (UV−vis) absorption spectra.[7,10,15] However, these structures cannot be unambiguously characterized.[11−16]

Non-contact atomic force microscopy (nc-AFM) with CO-functionalized tips has been used to characterize a wide range of organic compounds in the past decade.[21,22] It has proven particularly useful for characterizing large aromatic molecules

Special Issue: 2021 Pioneers in Energy Research: Alan Marshall

Received: July 22, 2021
Published: September 17, 2021

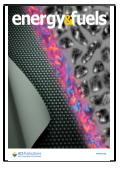

https://doi.org/10.1021/acs.energyfuels.1c02487
Energy Fuels 2021, 35, 18210−18219

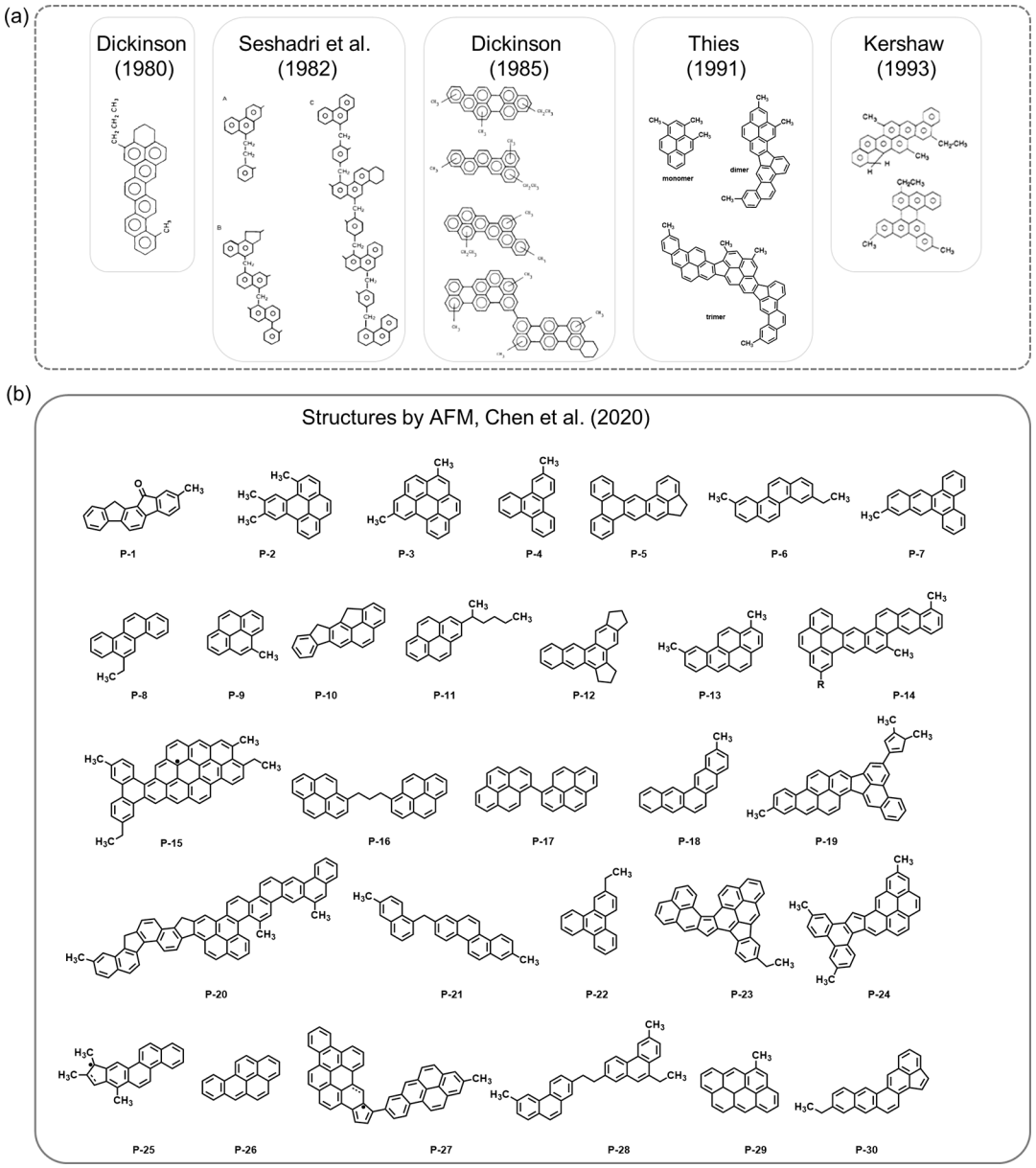

Figure 1. Various structural representions of M-50 pitch(a) and structuctures characterized with nc-AFM (b) by Chen et al. Average structures proposed by Dickinson. Reproduced with permission from refs 2 and 4. Copyrights 1980 and 1985 Elsevier, respectively. Average structure proposed by Seshadri et al. Reproduced with permission from ref 3. Copyright 1982 Elsevier. Average structure proposed by Kershaw and Black. Reproduced with permission from ref 6. Copyright 1993 American Chemical Society. Average structure proposed by Thies et al. Reproduced with permission from ref 10. Copyright 1991 Elsevier. Structures characterized with nc-AFM by Chen et al.[20] Reproduced with permission from ref 20. Copyright 2020 Elsevier.

of low solubility[23−25] and for directly identifying individual structures in complex mixtures.[26−30] This technique has been applied to characterize petroleum asphaltenes[31,32] and various fractions from heavy oils.[33−35] Studies using a model compound have been conducted to understand nonplanar conformations and heteroatom-containing components in petroleum as well.[36−40]

Recently, we applied nc-AFM to characterize M-50 pitch, and a great diversity of structures were revealed.[20] As shown in Figure 1b, many structural features predicted from previous characterizations can finally be confirmed yet with noticeable differences. For example, the predominance of methyl groups is observed, with a few larger alkyl substituents or side chains as well (e.g., P-8, P-11, and P-23), albeit with a wider range of their distributions than predicted. The presence of ring-joining methylene groups (Figures 1a and 2) predicted by Kershaw and Black was confirmed,[6] although they are less frequent than predicted (one in two molecules on average). The non-alternant PAHs fused by a conjugated five-membered ring predicted by Thies et al. have also been observed.[7,10,15] In addition, five- or six-membered alicyclic moieties fused to PAHs were observed (Figure 2). Single linkages via aryl−aryl bonds or an aliphatic (methylene or propylene) chain were observed, albeit rarely, and such structures were verified with atomic force microscopy (AFM) studies of bispyrene model compounds.[37,40] Overall, most molecules observed fall within the molecular weight range of 372.9 ± 138.0 Da, with an H/C

https://doi.org/10.1021/acs.energyfuels.1c02487
Energy Fuels 2021, 35, 18210−18219

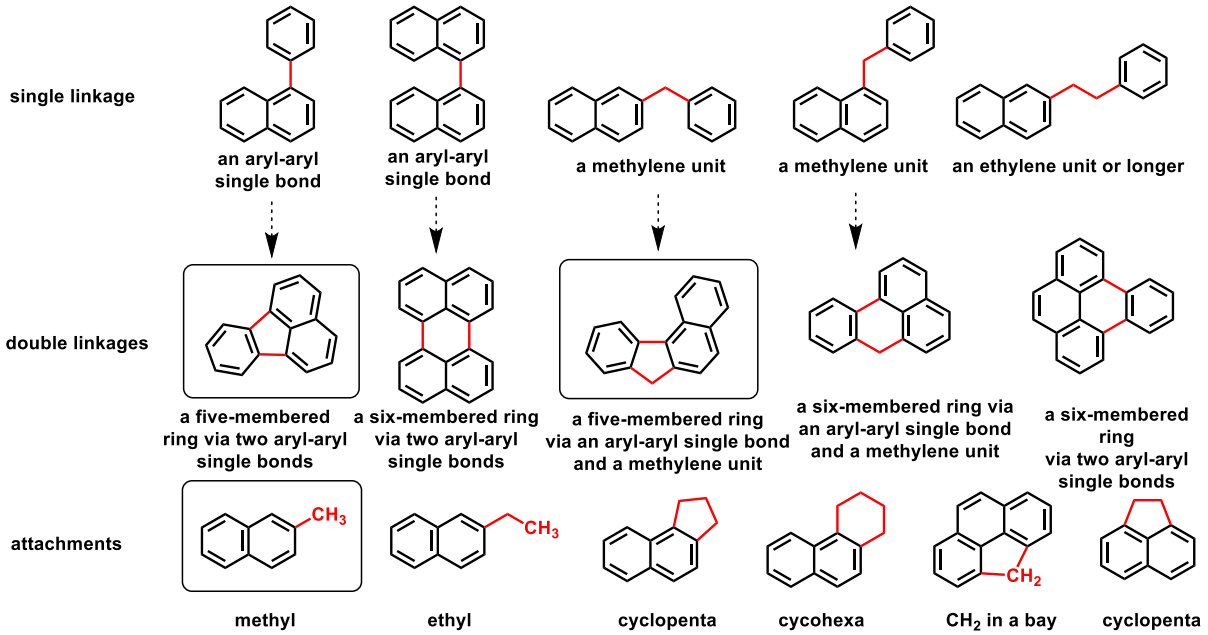

Figure 2. Some main structural features (in red) identified in M-50 pitch, including a single linkage (aryl−aryl single bond, methylene, ethylene, etc.) or double linkages (two aryl−aryl single bonds or one aryl−aryl plus a methylene linker) between two aromatic cores, and various moieties attached to an aromatic core, including methyl or ethyl side chains, cyclopenta or cyclohexa moieties, or a CH_2 unit inserted into the bay region. The dashed arrows designate related structures. Benzene or naphthalene are used to represent aryl groups. Some key structures discussed in this paper are enclosed in boxes.

ratio of 0.71 (0.73 from elemental analsysis), and most PAHs in the size of 4−12 rings.[20]

With structures of M-50 pitch characterized, many new questions emerge on how these molecules react to produce carbon materials. It is widely accepted that M-50 pitch undergoes a series of physical and chemical transformations to produce mesophase pitch when heated within the temperature range of 350−500 °C.[41] These structures grow larger through oligomerization and polymerization of individual starting molecules (or monomers), and eventually high-molecular-weight materials or coke will result upon further heating and/or carbonizing. Substantial evidence from studies by Lewis, Singer, and Greinke have suggested that the monomers are oligomerized via the formation of aryl−aryl single bonds[17,18,42−44] and that dealkylation and dehydrogenative coupling were suggested to be the main reactions during the continuous increase of the molecular weight (Figure 2).[17,45,46] The mechanisms involved in the formation of the intermediate mesophase state have received tremendous interest and have been studied extensively, including those involving free radicals as reactive intermediates as well as persistent species.[41,46−49]

However, most of these findings were based on the use of model aromatic hydrocarbons.[17,18,42−46] The study of petroleum pitch transformation remains a great challenge today as a result of the structural heterogeneity of the starting material, the many concurrent and parallel reactions that the material can undergo, and the decreased solubility of the reaction products in organic solvents with the growth in the molecular weight.[17,18,42,43,45,47] Hence, this study sought to better understand the mechanism of polymerization of M-50 pitch using nc-AFM to compare the structures of the polymerization products from two different approaches to those of the reactants shown in Figure 1. In the *ex situ* approach, structures produced from the thermal treatment of M-50 pitch at 400 °C for 3 or 6 h under a N_2 atmosphere are characterized by nc-AFM. In the *in situ* approach, reaction products from M-50 feed are induced by a brief thermal treatment (100−700 °C for 10−30 s) on an atomically clean Cu(111) surface in vacuum and then characterized by nc-AFM.

2. EXPERIMENTAL SECTION

2.1. Methods. *2.1.1. Thermal Treatment of M-50 Pitch (Ex Situ).* The thermally treated M-50 sample was prepared by loading a glass vial with ∼2 g of material and placed in a PAC micro carbon residue tester. The sample was heated to 100 °C within 10 min under a flow of nitrogen (600 mL/min). Immediately afterward, the sample was heated to 400 °C using a 30 °C/min ramp rate and 600 mL/min nitrogen flow rate. Upon reaching 400 °C, the flow rate was decreased to 150 mL/min and the sample was held at 400 °C for 3 or 6 h. After this condensed phase thermal treatment (also called heat soak), the sample was cooled to ambient temperature under nitrogen at a 600 mL/min flow rate over the course of several hours. The solid products after the thermal treatment were removed from the vial and characterized.

2.1.2. Thermogravimetric Analysis (TGA). PerkinElmer Pyris 1 TGA with a mass resolution of 0.1 μg was used for all thermogravimetric analyses. Approximately 10 mg of sample was loaded into a staged platinum pan, and the temperature was scanned from 30 to 950 °C with a ramp rate of 10 °C/min under a high-purity dried nitrogen (99.9995%) flow of 40 mL/min. Prior to thermal scanning, the sample was allowed to equilibrate in the staged pan under nitrogen for 30 min to ensure an established inert environment.

2.1.3. AFM Imaging. nc-AFM was carried out with low-temperature ultrahigh vacuum scanning tunneling microscopy/atomic force microscopy (LT UHV STM/AFM, CreaTec Fischer & Co., GmbH, Germany) operated under 4.8 K and ultrahigh vacuum (∼10^{-10} mbar). AFM images were obtained with a CO-functionalized tip in the frequency-modulated mode.[21] The sample was deposited onto a Cu(111) substrate via the resistive heating method.[37]

2.1.4. On-Surface Reaction (In Situ). M-50 pitch was deposited onto a Cu(111) surface with a higher coverage (∼0.5) and confirmed with STM and AFM. With the tip removed, the temperature of the Cu(111) substrate was quickly increased to ∼200−400 °C via

https://doi.org/10.1021/acs.energyfuels.1c02487
Energy Fuels 2021, 35, 18210−18219

resistance heating and held for 10−30 s (as specified in the text) before the heating was turned off. The substrate and sample were then cooled again to 4.8 K to be imaged with nc-AFM (section 3.3). The calibrated temperature control was around ±50 °C.

3. RESULTS AND DISCUSSION

3.1. Analysis of Products with TGA after Thermal Treatment of M-50 Pitch. After the condensed phase thermal treatment of M-50 pitch at 400 °C for 3 or 6 h under nitrogen, the formation of products with increased molecular weights is supported by the analysis of TGA data (Figure 3).

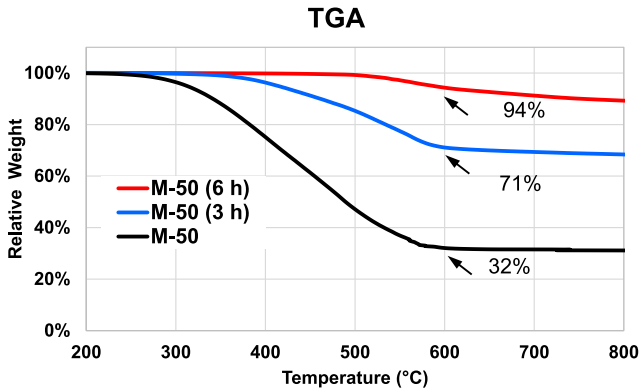

Figure 3. TGA of M-50 pitch and the products after thermal treatments at 400 °C for 3 or 6 h.

The relative residual weights of samples decrease upon increasing the temperatures to >300 °C under N_2 flow as a result of the evaporation of volatile molecules. The weight continues to decrease largely as a result of thermal cracking and evolution of gaseous molecules, and then the weight remains stable and constant at >600 °C. The residual stable weight is only 32% for M-50 pitch but increases to 71% for 3 h and 94% for 6 h of thermal treatment, respectively (Figure 3). This indicates that, after thermal treatments, most of the M-50 pitch molecules have been transformed into non-volatile structures with higher molecular weights.

A significant change in solubility was also noticed upon thermal treatment. While untreated M-50 pitch is readily soluble in the organic solvent chloroform and remains mostly soluble in chloroform after 3 h, most is insoluble after 6 h of thermal treatment. This is consistent with structures of high molecular weights. However, it poses challenges for most solution-based NMR and chromatographic techniques. Therefore, on the basis of our previous characterization of M-50 with nc-AFM,[20] we applied nc-AFM to characterize the structures of condensed phase reaction products from heat-treating M-50. We chose to image the thermal products after heating to 400 °C for 3 h instead of 6 h because the early events and the primary products from the initial chemical transformations are essential for understanding how these molecules react. The products after 6 h of thermal treatment will be complicated by secondary reactions (reactions of initial products).

3.2. nc-AFM Imaging of the Thermalized Products (*Ex Situ*). The thermal products (3 h at 400 °C) were introduced into nc-AFM via the flash heating method onto a Cu(111) surface at 4.8 K under ultrahigh vacuum. The molecules were characterized by nc-AFM with a CO-functionalized tip, and about 30 images were obtained (Figure 4). The planar aromatic structures composed of completely sp^2 carbons can be easily recognized in all images. The frequently observed protruding features in most images can be readily assigned to sp^3 carbon of a methyl group (molecules M-2, M-7, M-10, M-15, M-18, and M-21 in Figure 4) or a methylene group (CH_2) in five-membered rings (M-9) as a result of a high contrast from the repulsive interactions with the CO molecule of the AFM tip. Most molecules were imaged at different tip heights, especially for nonplanar structures or structural subregions (e.g., M-1, M-2, M-3, M-4, and M-5 in Figures S1−S3 of the Supporting Information). Assignment of these structures is confirmed by comparison to images of nonplanar moieties studied previously.[20,31,33,34,36,38,40]

Some images contain a dark region in part of the planar aromatic structures (e.g., M-1, M-3, M-6, and M-25). This is likely caused by a radical center as a result of the attractive interaction (hence, a darker contrast) between the CO tip and a free radical with unfilled molecular orbitals [singly occupied molecular orbital (SOMO)] and the fact that the PAH π-free radicals can often be delocalized in conjugated aromatic structures. Free radicals have also been observed in M-50 pitch by nc-AFM and reported previously.[20,50] To confirm this, we applied a voltage of ∼2 V using the AFM tip.[36,51,52] As shown in Figure 5, the CH_2 group and the surrounding region in structure M-9 were transformed into a darker region upon applying the electric pulse. This confirms both the presence of CH_2 in a five-membered ring and that the darker region is caused by the presence of a free radical resulting from the breakage of a C−H bond. Hence, the dark regions in a few molecules (M-1, M-3, M-6, and M-25) can be reasonably assigned to free radicals. It is interesting to note that the delocalization of the π radical is not delocalized to the whole PAH across the conjugated five-membered rings in a few molecules.

Comparing these structures (Figure 6) to those previously determined for M-50 pitch (Figure 1b)[20] reveals some significant differences. Most molecules are in the 300−800 g/mol molecular weight range, with a number-average molecular weight of 509 g/mol (Table S1 of the Supporting Information). The change in the molecular formula on average from $C_{24}H_{17}$ for M-50 pitch[20] to $C_{40}H_{25}$ for products clearly indicates the growth of the molecular weight by thermal treatments. Most structures contain an aromatic core with predominantly methyl groups as their side chains and very few long aliphatic chains. Aromatic cores connected by an aliphatic linker of more than one carbon were not observed, while some were observed in M-50 pitch. A few observed structures (M-1, M-5, M-23, M-25, and M-30) contain a single aryl−aryl bond, but more frequently, aromatic cores are bridged by a CH_2 unit in a non-conjugated five-membered ring (e.g., M-6, M-8, M-9, M-11, M-20, M-22, and M-26) or occasionally via a non-conjugated six-membered ring (e.g., M-11 and M-27). A carbonyl (C═O) group in a five-membered ring can also be found, but they can be considered as a product from a precursor with the CH_2 unit. Additionally, two aromatic cores are also frequently joined by a conjugative five-membered ring via two aryl−aryl single bonds (e.g., M-7, M-9, M-14, M-15, M-18, M-26, and M-28). Five- or six-membered alicyclic moieties fused to aromatic structures were also observed (M-3, M-6, M-13, and M-16), of which the presence can be confirmed by comparing nc-AFM images to those of model compounds.[36] A combination of several different features is frequently found in the same structure (M-6, M-8, and M-9).

https://doi.org/10.1021/acs.energyfuels.1c02487
Energy Fuels 2021, 35, 18210−18219

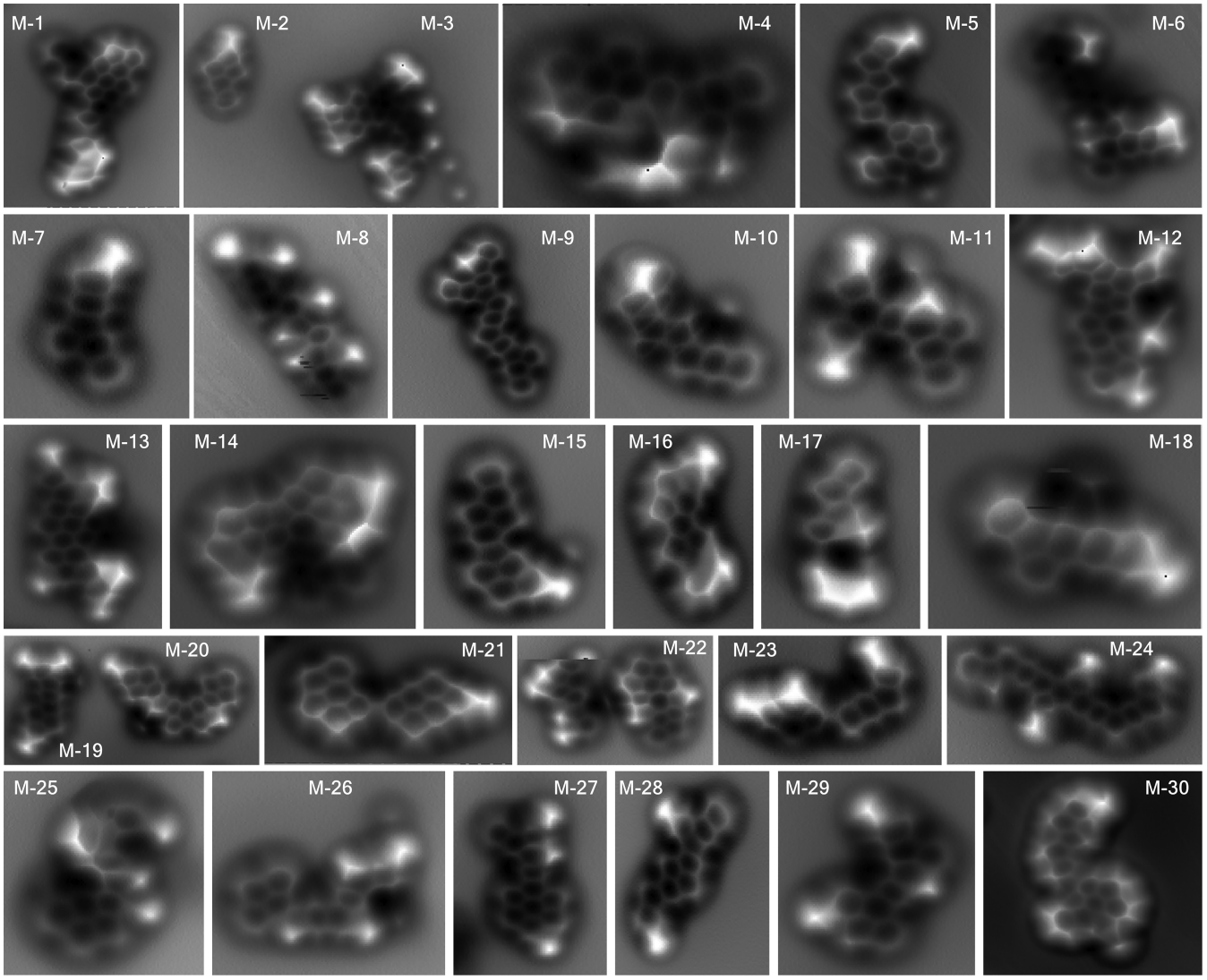

Figure 4. nc-AFM images on mesophase products (M-1−M-30) after thermal treatment of M-50 at 400 °C for 3 h show an increase in the molecular weight, with larger PAHs and fewer methyl groups than reactant M-50 molecules.

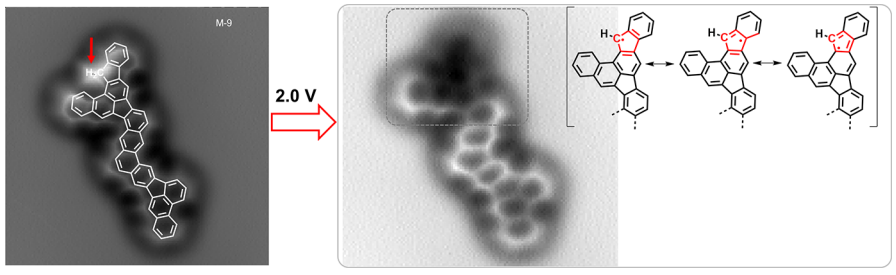

Figure 5. Confirmation of free radicals by breaking the C−H bond of molecule M-9 by applying an electric pulse (2 V) with the AFM tip (indicated by the red arrow). The darker region is due to the delocalization of the free radical by conjugation.

Both alternant and non-alternant PAHs are observed. The aromatic structures are predominantly composed of six- and five-membered aromatic rings. Other rings are extremely rare but, nevertheless, were observed, such as a seven-membered ring in M-22. Many PAHs are *cata*-condensed (e.g, M-8, M-9, and M-24) in a prolate shape, with fewer *peri*-condensed PAHs in an oblate shape, despite the greater thermodynamic stability of the *cata*-condensed aromatic structures (as a result of their higher concentration of Clar sextets).[39] The *cata*-condensed PAHs still follow the rule of three because the kinked structures are more stable.[35] A few free radicals are also observed, all delocalized π radicals (e.g., M-1, M-5, M-25, and M-30), and they seem to be more abundant than free radicals in the parent M-50 pitch.

Because very different structures are present in the products versus the reactant M-50 pitch, it is impossible to trace the reaction pathways by identifying which molecules are unreacted structures versus product molecules (reaction

https://doi.org/10.1021/acs.energyfuels.1c02487
Energy Fuels 2021, 35, 18210−18219

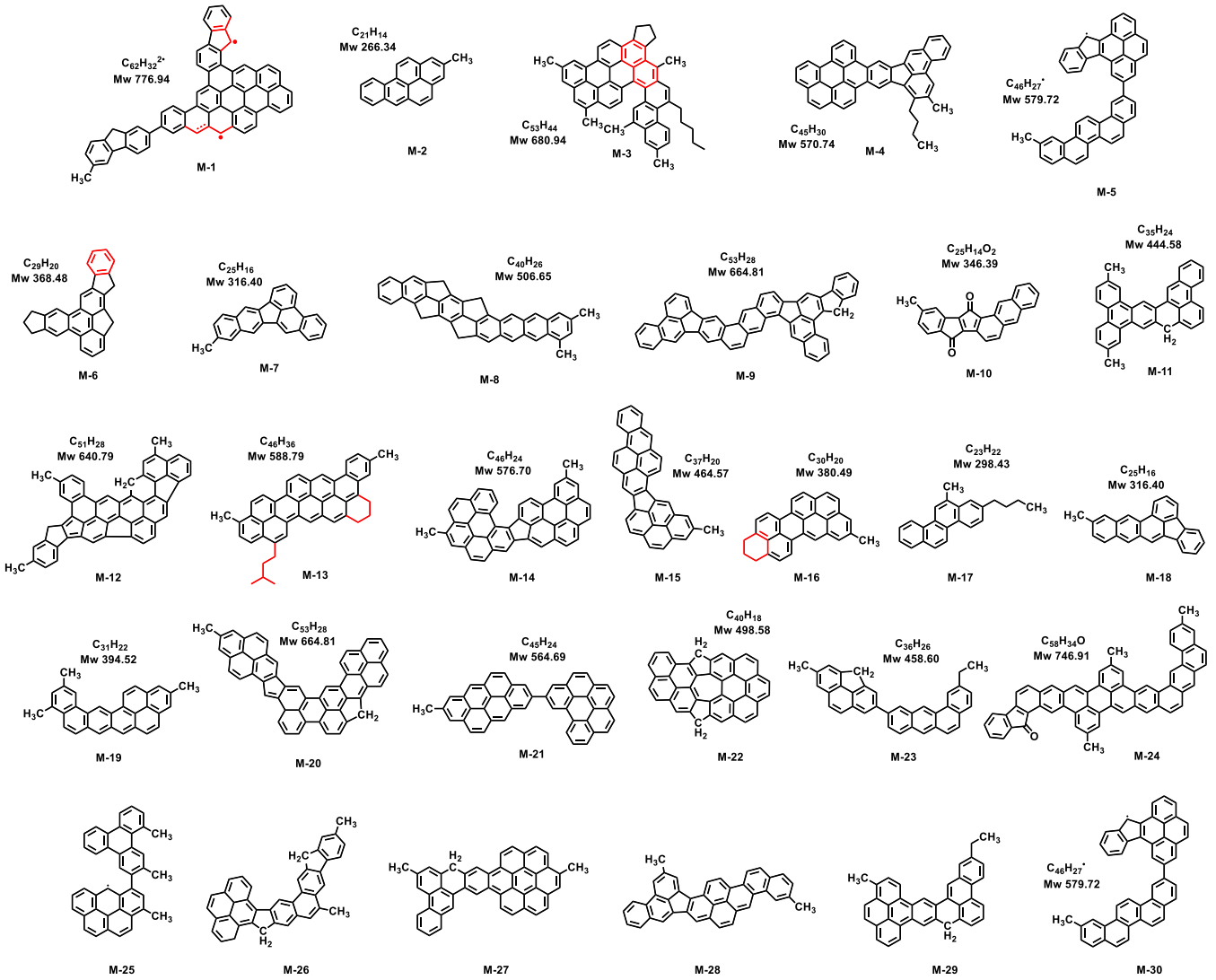

Figure 6. Chemical structures of products (M-1−M-30) from the thermal treatment of M-50 pitch from nc-AFM imaging shown in Figure 4. Ambiguous structural motifs are indicated in red.

expected to be incomplete after only 3 h) and how a specific structure is produced from its precursor molecules. Overall, molecules in the product are consistently larger than the PAHs observed in M-50 pitch, consistent with the expected molecular weight growth and polymerization during pyrolysis. Although methyl groups are still frequent and seem to predominate over longer alkyl groups in the products, there are fewer groups per structure compared to M-50 pitch. Coupled with the observation that the aromatic structures have grown larger than those in M-50, we postulate that polymerization is occurring via the consumption of methyl groups, potentially through coupling reactions.

3.3. Monitoring the On-Surface Reaction with nc-AFM (*In Situ*). We can monitor the reactions of M-50 pitch on a Cu(111) surface with nc-AFM. After the structures of M-50 pitch were imaged by nc-AFM at 4.8 K, the molecules were heated briefly (typically 10−30 s) by increasing the temperature of the Cu(111) surface to about 200 °C. As a result of catalysis by the atomically clean single-crystal Cu(111) surface, the as-synthesized product molecules can be imaged with nc-AFM after decreasing the temperature back to liquid helium temperatures. Four such images are shown in Figure 7a, and four more images of different regions were obtained after further reaction by heating to 400 °C (10 s) (Figure 7b). These latter images are of different regions than those of the former because it was not possible to monitor the same region throughout the heating and imaging cycles.

Reactions are evident as extremely large macromolecules were formed and covering the surface. Each imaged region is mostly planar and contains at least 200−400 atoms in the covalent bonding network. The structures are expected to interact strongly with the Cu surface or even to bind with the metal atoms via radical centers. The protruding features caused by methyl and methylene groups are still observed but significantly reduced. This indicates methyl group participation in the reactions connecting molecules, resulting in their incorporation into the aromatic structures. Upon additional heating (Figure 7b), the condensed structures are almost completely planar and devoid of methyl/methylene or aliphatic groups, with carbon atoms more densely connected. However, five-membered rings are still present in the product, as defects in the tightly connected and well-organized six-membered aromatic system.

https://doi.org/10.1021/acs.energyfuels.1c02487
Energy Fuels 2021, 35, 18210−18219

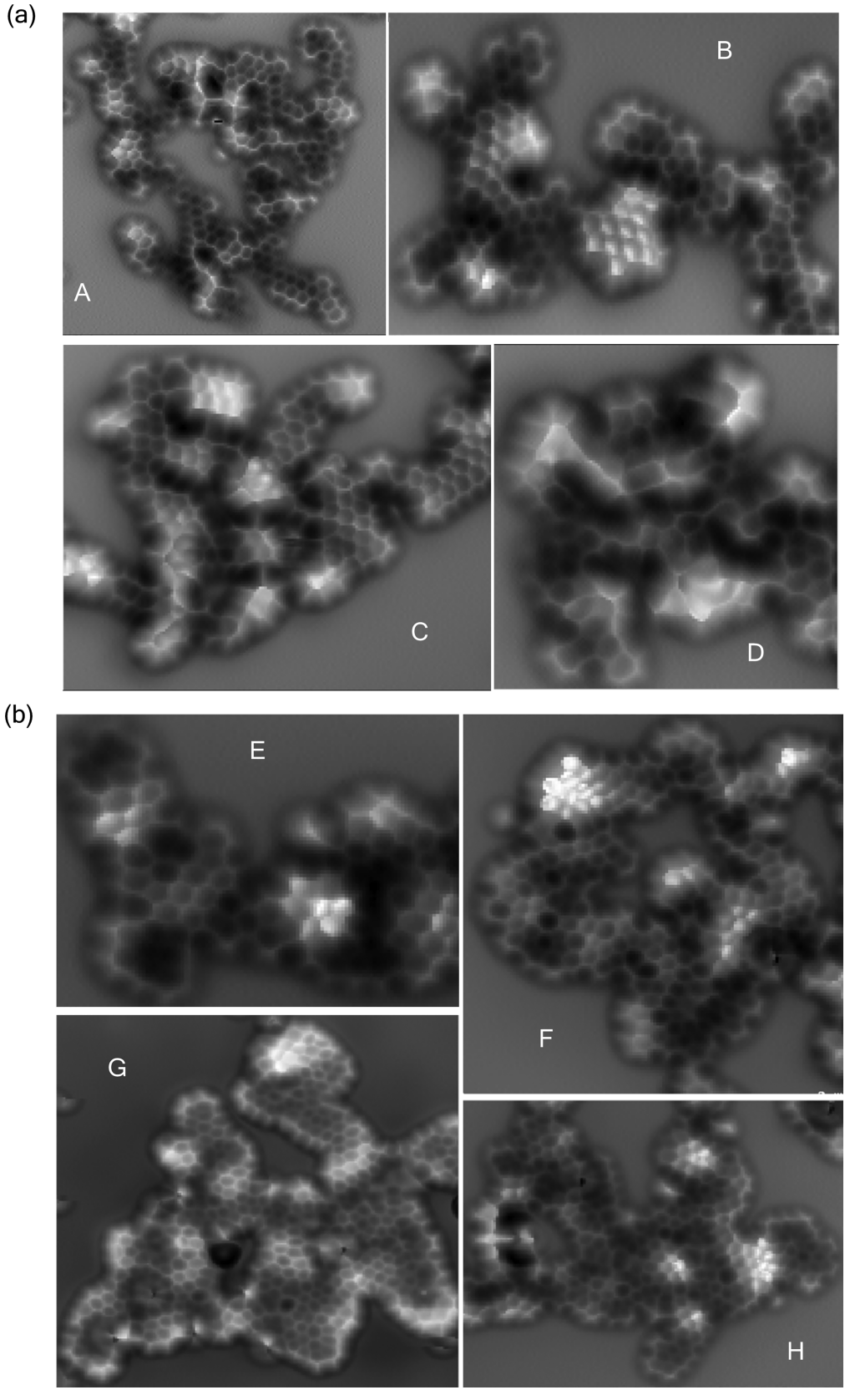

Figure 7. AFM images of an on-surface synthesized product from M-50 pitch heated to (a) 200 °C for 10 s (A–D) and after further heating at (b) 400 °C for 10 s (E–H). Size of each image ($w \times h$, nm): (A) 6.5 × 6.5, (B) 6.2 × 4, (C) 6.0 × 5.0, (D) 3.6 × 3.6, (E) 4.5 × 3.0, (F) 5.5 × 5.5, (G) 8 × 8, and (H) 7 × 5.3.

By comparison of the product molecules from the *ex situ* and *in situ* thermal treatments to the structures of M-50 pitch, it is clear that methyl groups in the starting materials were consumed during the reactions. Hence, methyl substituents

https://doi.org/10.1021/acs.energyfuels.1c02487
Energy Fuels 2021, 35, 18210–18219

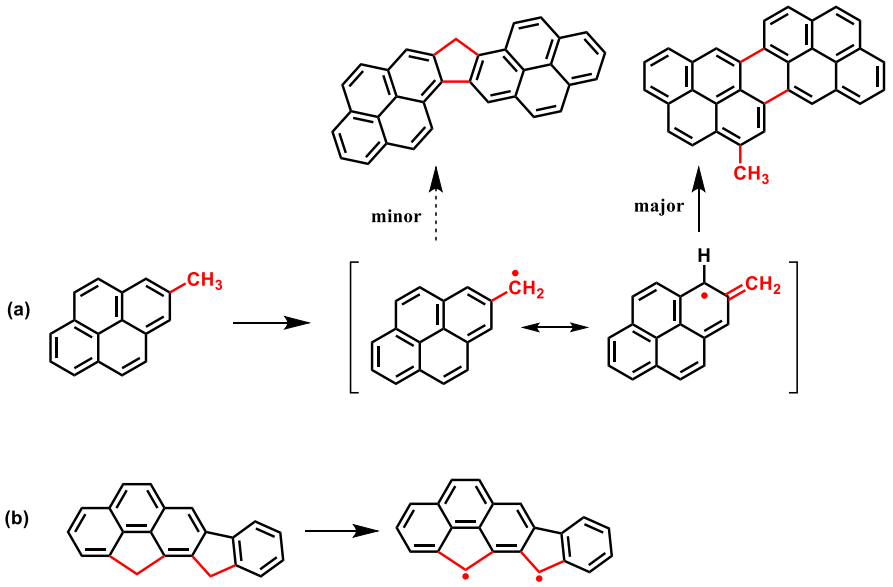

Figure 8. Proposed initial reaction steps in the generation of free radicals (a) from the methyl substituents of aromatic compounds and (b) from the five-membered rings containing a CH_2 unit.

can be considered as important cross-linking reagents to join two molecules. In addition, five-membered rings were still observed and prevalent in the products, and they seem to be formed or preserved during thermal reactions.

In previous work, a mechanism on the formation of M-50 pitch has been proposed.[20] In a subsequent study with dimethyl pyrene,[53] methyl groups were confirmed to initiate the coupling though six-membered rings via a resonance-stabilized π radical instead of a benzylic radical, which would result in a structure bridged by a five-membered ring. On the basis of these previous studies, we propose the following initial reactions in the polymerization of M-50 pitch molecules to form higher molecular weight carbon materials (Figure 8).

The primary benzylic free radical after cleavage of the C−H bond in the methyl-substituted PAHs is stabilized by conjugation with the PAH system. Other molecules with aliphatic substituents longer than methyl should react similarly to benzylic radicals by breaking the weak C−C or C−H bond. As shown in the previous study with dimethylpyrene,[53] the major reaction pathway for this benzylic radical is via its resonance π-radical structure to form a product joined by a six-membered ring instead of a direct reaction via the benzylic radical to produce products joined by a non-conjugated five-membered ring. Similarly, the bond dissociation energy (BDE) of the benzylic C−H bond in the CH_2 unit in a five-membered ring is only about ∼75 kcal/mol,[54] significantly weaker than those in alkanes (103 kcal/mol in methane) or aromatic rings (110 kcal/mol in benzene). Hence, we predict that such structures with a CH_2 unit can be either a good radical initiator during the early reaction events by breakage of the weakest C−H bond under thermal conditions or as a radical sink in the later reactions by providing a H radical to the more reactive radicals remaining. The complete reaction pathways of the five-membered rings are not yet clear, and further work is ongoing.

4. CONCLUSION

Pitches derived from petroleum or coal tar are cheap and abundant feedstocks to make advanced carbon materials when compared to synthetic polymers (polyacrylonitrile), natural polymers (rayon), or synthetic pitches derived from petrochemicals, such as naphthalene or anthracene. Tremendous amounts of research have been devoted to characterizing the molecules in M-50 petroleum pitch and understanding the mechanisms of mesophase formation and carbonization, although significant unknowns remain. Recently, we characterized structures of M-50 pitch molecules with the state-of-the-art nc-AFM technique[20] and identified common structural features scattered (often contradictory) in previous reports. To confirm these results, dimethylpyrene (DMPY) was designed to mimic the predominant methyl groups in M-50 pitch.[53] Results from DMPY confirmed that the mesophase formation and characterization of the thermal products with nc-AFM revealed unexpected major coupling reaction pathways via the π-radical intermediate. As a continuation of these previous studies, we extend this work toward understanding the mechanism of molecular weight growth and polymerization reactions of M-50 by comparing the *ex situ* condensed phase thermal reaction to the *in situ* on-surface reactions. The decrease in methyl groups and growth of molecular weight in both reactions confirmed the previous hypothesis that methyl groups play an important role in M-50 pitch. However, it is worth noting that these results should only be understood in the context of M-50 pitch and the specific reactions that it undergoes under thermal conditions, and they do not exclude other potential reaction pathways. For example, pitches derived from precursors without methyl groups, such as pyrene, anthracene, or naphthalene, have been made under other reaction conditions. These systemic studies represent a major step in understanding the key structural features in M-50 and the mechanism of mesophase formation under thermal conditions. Other functional groups and structural units, such as PAH structures, two types of five-membered rings, and/or specific aromatic catenation or substitution patterns, may also be important, although they are not yet well-understood.

https://doi.org/10.1021/acs.energyfuels.1c02487
Energy Fuels 2021, 35, 18210−18219

■ ASSOCIATED CONTENT

Supporting Information

The Supporting Information is available free of charge at https://pubs.acs.org/doi/10.1021/acs.energyfuels.1c02487.

AFM images of the structure with different tip heights (Figures S1−S3) and list of compounds in products from *ex situ* thermal treatment of M-50 pitch by nc-AFM (Table S1) (PDF)

■ AUTHOR INFORMATION

Corresponding Authors

Nan Yao − *Andlinger Center for Energy and the Environment, Princeton University, Princeton, New Jersey 08540, United States*; Email: nyao@princeton.edu

Yunlong Zhang − *Corporate Strategic Research, ExxonMobil Research and Engineering Company, Annandale, New Jersey 08801, United States*; orcid.org/0000-0002-3071-8625; Email: yunlong.zhang@exxonmobil.com

Authors

Pengcheng Chen − *Andlinger Center for Energy and the Environment, Princeton University, Princeton, New Jersey 08540, United States*

Jordan N. Metz − *Corporate Strategic Research, ExxonMobil Research and Engineering Company, Annandale, New Jersey 08801, United States*

Adam S. Gross − *Corporate Strategic Research, ExxonMobil Research and Engineering Company, Annandale, New Jersey 08801, United States*

Stuart E. Smith − *Corporate Strategic Research, ExxonMobil Research and Engineering Company, Annandale, New Jersey 08801, United States*

Steven P. Rucker − *Corporate Strategic Research, ExxonMobil Research and Engineering Company, Annandale, New Jersey 08801, United States*

Complete contact information is available at: https://pubs.acs.org/10.1021/acs.energyfuels.1c02487

Notes

The authors declare no competing financial interest.

■ ACKNOWLEDGMENTS

This is a submission to the special issue of 2021 Pioneers in Energy Research honoring Dr. Alan Marshall. The authors thank him for his tremendous contributions to petroleum characterization and for being an inspiring role model for young researchers. Comments and revision of the manuscript by Michael Siskin are gratefully acknowledged. The authors also acknowledge the use of Princeton's Imaging and Analysis Center, which is partially supported by the Princeton Center for Complex Materials, a National Science Foundation (NSF)−Materials Research Science and Engineering Center (MRSEC) Program (DMR-2011750).

■ REFERENCES

(1) Smith, W. E.; Horne, O. J., Jr.; Napier, B., Jr. *Characterization and Reproducibility of Petroleum Pitches*; Oak Ridge Y-12 Plant: Oak Ridge, TN, March 3, 1974; Technical Report Y-1921, DOI: 10.2172/4330482.

(2) Dickinson, E. M. Structural comparison of petroleum fractions using proton and ^{13}C n.m.r. spectroscopy. *Fuel* **1980**, *59* (5), 290−294.

(3) Seshadri, K. S.; Bacha, J. D.; Albaugh, E. W. Structural characterization of fractions of petroleum pitch and ethylene pyrolysis tar by proton and carbon-13 NMR spectroscopy. *Fuel* **1982**, *61* (11), 1095−100.

(4) Dickinson, E. M. Average structures of petroleum pitch fractions by proton/carbon-13 NMR spectroscopy. *Fuel* **1985**, *64* (5), 704−6.

(5) Hutchenson, K. W.; Roebers, J. R.; Thies, M. C. Fractionation of petroleum pitch with supercritical toluene. *J. Supercrit. Fluids* **1991**, *4* (1), 7−14.

(6) Kershaw, J. R.; Black, K. J. T. Structural characterization of coal-tar and petroleum pitches. *Energy Fuels* **1993**, *7* (3), 420−5.

(7) Burgess, W. A.; Pittman, J. J.; Marcus, R. K.; Thies, M. C. Structural Identification of the Monomeric Constituents of Petroleum Pitch. *Energy Fuels* **2010**, *24* (8), 4301−4311.

(8) Edwards, W. F.; Jin, L.; Thies, M. C. MALDI-TOF mass spectrometry: Obtaining reliable mass spectra for insoluble carbonaceous pitches. *Carbon* **2003**, *41* (14), 2761−2768.

(9) Cristadoro, A.; Kulkarni, S. U.; Burgess, W. A.; Cervo, E. G.; Raeder, H. J.; Muellen, K.; Bruce, D. A.; Thies, M. C. Structural characterization of the oligomeric constituents of petroleum pitches. *Carbon* **2009**, *47* (10), 2358−2370.

(10) Burgess, W. A.; Thies, M. C. Molecular structures for the oligomeric constituents of petroleum pitch. *Carbon* **2011**, *49* (2), 636−651.

(11) Kulkarni, S. U.; Räder, H. J.; Thies, M. C. The effects of molecular weight distribution and sample preparation on matrix-assisted laser desorption/ionization time-of-flight mass spectrometric analysis of petroleum macromolecules. *Rapid Commun. Mass Spectrom.* **2011**, *25* (19), 2799−2808.

(12) Kulkarni, S. U.; Esguerra, D. F.; Thies, M. C. Isolating Petroleum Pitch Oligomers via Semi-continuous Supercritical Extraction. *Energy Fuels* **2012**, *26* (5), 2721−2726.

(13) Esguerra, D. F.; Hoffman, W. P.; Thies, M. C. Fractionation of an oligomeric pyrene pitch via supercritical extraction. *J. Supercrit. Fluids* **2013**, *79*, 170−176.

(14) Esguerra, D. F.; Hoffman, W. P.; Thies, M. C. Liquid crystallinity in trimer oligomers isolated from petroleum and pyrene pitches. *Carbon* **2014**, *79*, 265−273.

(15) Thies, M. C. Fractionation and Characterization of Carbonaceous Pitch Oligomers: Understanding the Building Blocks for Carbon Materials. In *Polymer Precursor-Derived Carbon*; Naskar, A. K., Hoffman, W. P., Eds.; American Chemical Society (ACS): Washington, D.C., 2014; ACS Symposium Series, Vol. *1173*, Chapter 5, pp 85−136, DOI: 10.1021/bk-2014-1173.ch005.

(16) Zhang, W.; Andersson, J. T.; Raeder, H. J.; Muellen, K. Molecular characterization of large polycyclic aromatic hydrocarbons in solid petroleum pitch and coal tar pitch by high resolution MALDI ToF MS and insights from ion mobility separation. *Carbon* **2015**, *95*, 672−680.

(17) Lewis, I. C.; Kovac, C. A. The role of free radicals and molecular size in mesophase pitch. *Carbon* **1978**, *16* (6), 425−9.

(18) Lewis, I. C. Thermal polymerization of aromatic hydrocarbons. *Carbon* **1980**, *18* (3), 191−6.

(19) Kim, B.-J.; Eom, Y.; Kato, O.; Miyawaki, J.; Kim, B. C.; Mochida, I.; Yoon, S.-H. Preparation of carbon fibers with excellent mechanical properties from isotropic pitches. *Carbon* **2014**, *77*, 747−755.

(20) Chen, P.; Metz, J. N.; Mennito, A. S.; Merchant, S.; Smith, S. E.; Siskin, M.; Rucker, S. P.; Dankworth, D. C.; Kushnerick, J. D.; Yao, N.; Zhang, Y. Petroleum pitch: Exploring a 50-year structure puzzle with real-space molecular imaging. *Carbon* **2020**, *161*, 456−465.

(21) Gross, L.; Mohn, F.; Moll, N.; Liljeroth, P.; Meyer, G. The Chemical Structure of a Molecule Resolved by Atomic Force Microscopy. *Science* **2009**, *325*, 1110−1114.

(22) Gross, L.; Mohn, F.; Moll, N.; Meyer, G.; Ebel, R.; Abdel-Mageed, W. M.; Jaspars, M. Organic structure determination using atomic-resolution scanning probe microscopy. *Nat. Chem.* **2010**, *2* (10), 821−825.

(23) Gross, L.; Mohn, F.; Moll, N.; Schuler, B.; Criado, A.; Guitian, E.; Pena, D.; Gourdon, A.; Meyer, G. Bond-Order Discrimination by Atomic Force Microscopy. *Science* **2012**, *337*, 1326−1329.
(24) Schuler, B.; Collazos, S.; Gross, L.; Meyer, G.; Perez, D.; Guitian, E.; Pena, D. From perylene to a 22-ring aromatic hydrocarbon in one-pot. *Angew. Chem., Int. Ed.* **2014**, *53* (34), 9004−9006.
(25) Vilas-Varela, M.; Fatayer, S.; Majzik, Z.; Pérez, D.; Guitián, E.; Gross, L.; Peña, D. [19]Dendriphene: A 19-Ring Dendritic Nanographene. *Chem. - Eur. J.* **2018**, *24* (67), 17697−17700.
(26) Fatayer, S.; Poddar, N. B.; Quiroga, S.; Schulz, F.; Schuler, B.; Kalpathy, S. V.; Meyer, G.; Perez, D.; Guitian, E.; Pena, D.; Wornat, M. J.; Gross, L. Atomic Force Microscopy Identifying Fuel Pyrolysis Products and Directing the Synthesis of Analytical Standards. *J. Am. Chem. Soc.* **2018**, *140* (26), 8156−8161.
(27) Fatayer, S.; Coppola, A. I.; Schulz, F.; Walker, B. D.; Broek, T. A.; Meyer, G.; Druffel, E. R. M.; McCarthy, M.; Gross, L. Direct Visualization of Individual Aromatic Compound Structures in Low Molecular Weight Marine Dissolved Organic Carbon. *Geophys. Res. Lett.* **2018**, *45* (11), 5590−5598.
(28) Commodo, M.; Kaiser, K.; De Falco, G.; Minutolo, P.; Schulz, F.; D'Anna, A.; Gross, L. On the early stages of soot formation: Molecular structure elucidation by high-resolution atomic force microscopy. *Combust. Flame* **2019**, *205*, 154−164.
(29) Schulz, F.; Commodo, M.; Kaiser, K.; De Falco, G.; Minutolo, P.; Meyer, G.; D'Anna, A.; Gross, L. Insights into incipient soot formation by atomic force microscopy. *Proc. Combust. Inst.* **2019**, *37* (1), 885−892.
(30) Schulz, F.; Maillard, J.; Kaiser, K.; Schmitz-Afonso, I.; Gautier, T.; Afonso, C.; Carrasco, N.; Gross, L. Imaging Titan's Organic Haze at Atomic Scale. *Astrophys. J., Lett.* **2021**, *908* (1), L13.
(31) Schuler, B.; Meyer, G.; Pena, D.; Mullins, O. C.; Gross, L. Unraveling the Molecular Structures of Asphaltenes by Atomic Force Microscopy. *J. Am. Chem. Soc.* **2015**, *137* (31), 9870−9876.
(32) Schuler, B.; Meyer, G.; Peña, D.; Mullins, O. C.; Gross, L. Unraveling the Molecular Structures of Asphaltenes by Atomic Force Microscopy. *J. Am. Chem. Soc.* **2015**, *137*, 9870.
(33) Schuler, B.; Fatayer, S.; Meyer, G.; Rogel, E.; Moir, M.; Zhang, Y.; Harper, M. R.; Pomerantz, A. E.; Bake, K. D.; Witt, M.; Pena, D.; Kushnerick, J. D.; Mullins, O. C.; Ovalles, C.; van den Berg, F. G. A.; Gross, L. Heavy Oil Based Mixtures of Different Origins and Treatments Studied by Atomic Force Microscopy. *Energy Fuels* **2017**, *31* (7), 6856−6861.
(34) Zhang, Y.; Schulz, F.; Rytting, B.; Walters, C.; Kaiser, K.; Metz, J.; Harper, M.; Merchant, S.; Mennito, A.; Qian, K.; Kushnerick, J.; Kilpatrick, P.; Gross, L. Elucidating the Geometric Substitution of Petroporphyrins by Spectroscopic Analysis and AFM Molecular Imaging. *Energy Fuels* **2019**, *33* (7), 6088−6097.
(35) Zhang, Y. Nonalternant Aromaticity and Partial Double Bond in Petroleum Molecules Revealed: Theoretical Understanding of Polycyclic Aromatic Hydrocarbons Obtained by Non-contact Atomic Force Microscopy. *Energy Fuels* **2019**, *33* (5), 3816−3820.
(36) Schuler, B.; Zhang, Y.; Collazos, S.; Fatayer, S.; Meyer, G.; Perez, D.; Guitian, E.; Harper, M. R.; Kushnerick, J. D.; Pena, D.; Gross, L. Characterizing aliphatic moieties in hydrocarbons with atomic force microscopy. *Chem. Sci.* **2017**, *8* (3), 2315−2320.
(37) Zhang, Y.; Schuler, B.; Fatayer, S.; Gross, L.; Harper, M. R.; Kushnerick, J. D. Understanding the Effects of Sample Preparation on the Chemical Structures of Petroleum Imaged with Noncontact Atomic Force Microscopy. *Ind. Eng. Chem. Res.* **2018**, *57* (46), 15935−15941.
(38) Zahl, P.; Zhang, Y. Guide for Atomic Force Microscopy Image Analysis To Discriminate Heteroatoms in Aromatic Molecules. *Energy Fuels* **2019**, *33* (6), 4775−4780.
(39) Zhang, Y. Identify Similarities in Diverse Polycyclic Aromatic Hydrocarbons of Asphaltenes and Heavy Oils Revealed by Non-contact Atomic Force Microscopy: Aromaticity, Bonding, and Implications in Reactivity. In *Chemistry Solutions to Challenges in the Petroleum Industry*; Rahimi, P., Ovalles, C., Zhang, Y., Adams, J., Eds.; American Chemical Society (ACS): Washington, D.C., 2019; ACS Symposium Series, Vol. *1320*, Chapter 3, pp 39−65, DOI: 10.1021/bk-2019-1320.ch003.
(40) Chen, P.; Joshi, Y. V.; Metz, J. N.; Yao, N.; Zhang, Y. Conformational Analysis of Nonplanar Archipelago Structures on a Cu (111) Surface by Molecular Imaging. *Energy Fuels* **2020**, *34* (10), 12135−12141.
(41) Greinke, R. A.; Singer, L. S. Constitution of coexisting phases in mesophase pitch during heat treatment: Mechanism of mesophase formation. *Carbon* **1988**, *26* (5), 665−670.
(42) Lewis, I. C. Chemistry of carbonization. *Carbon* **1982**, *20* (6), 519−29.
(43) Lewis, I. C. Chemistry of pitch carbonization. *Fuel* **1987**, *66* (11), 1527−1531.
(44) Greinke, R. A.; Lewis, I. C. Carbonization of naphthalene and dimethylnaphthalene. *Carbon* **1984**, *22* (3), 305−314.
(45) Singer, L. S.; Lewis, I. C. ESR study of the kinetics of carbonization. *Carbon* **1978**, *16* (6), 417−23.
(46) Greinke, R. A. Kinetics of petroleum pitch polymerization by gel permeation chromatography. *Carbon* **1986**, *24* (6), 677−686.
(47) Greinke, R. A.; Lewis, I. C. Pyrolysis studies on model aromatic sulfur compounds. *Carbon* **1979**, *17* (6), 471−7.
(48) Mochida, I.; Korai, Y.; Ku, C.-H.; Watanabe, F.; Sakai, Y. Chemistry of synthesis, structure, preparation and application of aromatic-derived mesophase pitch. *Carbon* **2000**, *38* (2), 305−328.
(49) Azami, K.; Yamamoto, S.; Sanada, Y. Carbonization behavior of petroleum pitch—In situ high-temperature ^{13}C-NMR measurements. *Carbon* **1993**, *31* (4), 611−615.
(50) Zhang, Y.; Siskin, M.; Gray, M. R.; Walters, C. C.; Rodgers, J. R. Mechanisms of Asphaltene Aggregation: Puzzles and a New Hypothesis. *Energy Fuels* **2020**, *34* (8), 9094−9107.
(51) Gross, L.; Schuler, B.; Pavlicek, N.; Fatayer, S.; Majzik, Z.; Moll, N.; Pena, D.; Meyer, G. Atomic Force Microscopy for Molecular Structure Elucidation. *Angew. Chem., Int. Ed.* **2018**, *57* (15), 3888−3908.
(52) Mistry, A.; Moreton, B.; Schuler, B.; Mohn, F.; Meyer, G.; Gross, L.; Williams, A.; Scott, P.; Costantini, G.; Fox, D. J. The Synthesis and STM/AFM Imaging of Olympicene Benzo[*cd*]pyrenes. *Chem. - Eur. J.* **2015**, *21* (5), 2011−2018.
(53) Chen, P.; Fatayer, S.; Schuler, B.; Metz, J. N.; Gross, L.; Yao, N.; Zhang, Y. The Role of Methyl Groups in the Early Stage of Thermal Polymerization of Polycyclic Aromatic Hydrocarbons Revealed by Molecular Imaging. *Energy Fuels* **2021**, *35* (3), 2224−2233.
(54) Zhang, X.-M.; Bordwell, F. G. Homolytic bond dissociation energies of the benzylic carbon-hydrogen bonds in radical anions and radical cations derived from fluorenes, triphenylmethanes, and related compounds. *J. Am. Chem. Soc.* **1992**, *114* (25), 9787−9792.